Relaxed control of sugar utilization in *Parageobacillus thermoglucosidasius* DSM 2542

Jinghui Liang[1], Adam Roberts[1], Richard van Kranenburg[2,3], Albert Bolhuis[4] and David Leak[1]

[1]Department of Biology and Biochemistry, University of Bath, UK
[2]Laboratory of Microbiology, Wageningen University, The Netherlands
[3]Corbion, Arkelsedijk 46, 4206 AC, Gorinchem, The Netherlands
[4]Department of Pharmacy and Pharmacology, University of Bath, UK

27th December 2021

Corresponding author

Name: Jinghui Liang
Address: 4 South 1.28, Department of Biology and Biochemistry, University of Bath, UK
Postcode: BA2 7AY
Email: jjl51@bath.ac.uk

Abstract

Though carbon catabolite repression (CCR) has been intensively studied in some more characterised organisms, there is a lack of information of CCR in thermophiles. In this work, CCR in the thermophile, *Parageobacillus thermoglucosidasius* DSM 2542 has been studied during growth on pentose sugars in the presence of glucose. Physiological studies under fermentative conditions revealed a loosely controlled CCR when DSM 2542 was grown in minimal medium supplemented with a mixture of glucose and xylose. This atypical CCR pattern was also confirmed by studying xylose isomerase expression level by qRT-PCR. Fortuitously, the *pheB* gene, which encodes catechol 2,3-dioxygenase was found to have a *cre* site highly similar to the consensus catabolite-responsive element (*cre*) at its 3′ end and was used to confirm that expression of *pheB* from a plasmid was under stringent CCR control. Bioinformatic analysis suggested that the CCR regulation of xylose metabolism in *P. thermoglucosidasius* DSM 2542 might occur primarily via control of expression of pentose transporter operons. Relaxed control of sugar utilization might reflect a lower affinity of the CcpA-HPr (Ser46-P) or CcpA-Crh (Ser46-P) complexes to the *cre*(s) in these operons.

Key words

Carbon catabolite repression; *Parageobacillus thermoglucosidasius*; *cre*; *pheB*; Redox

1 Introduction

Carbon catabolite repression (CCR) is a regulatory system found in many microbes, in which the expression of certain catabolic genes is repressed in the presence of more rapidly metabolizable carbon sources, typically glucose, fructose or mannitol (Hueck and Hillen, 1995; Kraus et al., 1994). In nature, CCR allows for the uptake of the most energy-efficient carbon sources prior to the others (Görke and Stülke, 2008). However, CCR can be a major bottleneck in lignocellulosic biomass fermentation. Lignocellulose mainly consists of cellulose, hemicellulose and lignin, of which the carbohydrates would be broken down into a mixture of hexose (C6) and pentose (C5) sugars including glucose, xylose and arabinose (Isikgor and Becer, 2015). Sequential consumption of sugars resulting from CCR makes the fermentation environment less controllable, extending the fermentation time and affecting the product yield of the fermentation process (Kim et al., 2010; Vinuselvi et al., 2012). Hence, being able to utilize hexoses and pentoses simultaneously during fermentation is a highly valuable trait for producing bio-derived products such as butanol, ethanol, lactic acid and succinic acid (Bechthold et al., 2008; Whitfield et al., 2012).

CCR exists in most known mesophilc bacteria, with *Lactobacillus brevis* as an exception (Kim et al., 2009). Curiously, recent studies suggested that CCR is absent from several thermophiles, such as *Caldicellulosiruptor saccharolyticus* (VanFossen et al., 2009), *Thermoanaerobacterium saccharolyticum* (Shaw et al., 2008) and *Thermoanaerobacter* sp. (L. Lin et al., 2011). These organisms can grow on xylan, xylo/gluco-oligosaccharide and monosaccharides (glucose, xylose, arabinose, mannose, galactose and fructose). *Thermoanaerobacter* sp. achieved this by simultaneous activation of catabolic pathways for all available sugars under the regulation of beta-glucoside (*bgl*) operon antiterminators of the BglG family, which is different from the catabolic machineries reported in model mesophilic organisms *Escherichia coli* and *Bacillis subtilis* (L. Lin et al., 2011). *C. saccharolyticus* was not subject to CCR because it does not possess the global regulatory system for carbohydrate utilization commonly found

in low G+C Gram-positive bacteria such as *B. subtilis*, *Lactococcus lactis*, and *Streptococcus pneumoniae* (VanFossen et al., 2009). *Parageobacillus* spp. are thermophiles which can utilize oligosaccharides and a wide range of monomeric sugars. Yet, to date, little information has been documented about the CCR in *Geobacillus* or *Parageobacillus* spp.

Parageobacillus spp. are Gram-positive, facultative anaerobes which can grow between 50°C and 70°C, with an optimum range of 60∼65 °C (Hills, 2015). A high temperature is beneficial for industrial fermentation as it can reduce the risk of contamination from typical contaminants and cuts down the cooling cost in this exothermic process (Junker et al., 2006). Besides, 55∼60°C is the typical temperature for enzymatic pre-treatment of biomass substrates, so growth at 60°C is compatible with continued hydrolysis (i.e. simultaneous saccharification and fermentation). *P. thermoglucosidasius* has attracted a lot of interest because of its potential industrial application (Hussein et al., 2015). It can efficiently utilize oligosaccharides, cellobiose, pentose and hexose sugars from various feedstocks including lignocellulosic biomass. It produces ethanol, lactate, formate and succinate as fermentation products (Hills, 2015). Several genetic tools and transformation procedures have been developed for the genetic manipulation of *P. thermoglucosidasius* (Bacon et al., 2017; Macklyne, 2017; Sheng et al., 2017), and these have been used to engineer *P. thermoglucosidasius* for production of, for instance, ethanol, lactic acid or isobutanol (Hills, 2015; P. P. Lin et al., 2014; Raita et al., 2016; Van Kranenburg et al., 2019).

P. thermoglucosidasius belongs to the family *Bacillaceae* and the phylum Firmicutes (Aliyu et al., 2016), in which a CcpA-dependent machinery has been demonstrated for CCR (Görke and Stülke, 2008). There are a few key players in this regulatory network, including the histidine-phosphocarrier protein (HPr), an HPr-like protein (Crh), the catabolic control protein (CcpA), and at a genetic level, the catabolite-responsive element (*cre*) (Singh et al., 2008). Glucose, which plays a central role in CCR, can be transported across the cell membrane and simultaneously converted into glucose-6-phosphate via the phosphoenolpyruvate:sugar phosphotransferase system (PTS) when the HPr is phosphorylated on its His-15 residue by Enzyme I (EI) of the PTS (Fig.1) (Görke and Stülke, 2008). During glycolysis, glucose-6-phosphate is converted into fructose-1,6-bisphosphate. The accumulation of glucose-6-phosphate and fructose-1,6-bisphosphate can stimulate HPr kinase (HPr) to phosphorylate both HPr and Crh on their Ser-46 residues (Warner and Lolkema, 2003a). Then, the HPr (Ser-P) or Crh (Ser-P) binds to CcpA and forms a CcpA-HPr (Ser46-P) or CcpA-Crh (Ser46-P) complex (Fujita, 2009; Galinier et al., 1999). Either the CcpA-HPr (Ser46-P) or CcpA-Crh (Ser46-P) complex can bind to one or more *cre* boxes located either upstream of, or within the genes, resulting in either up- or down-regulation of expression of these genes, respectively (Inácio et al., 2003). If a *cre* box is located upstream of the -35 region of the promoter, binding of the CcpA-HPr (Ser46-P) or CcpA-Crh (Ser46-P) complex can result in either catabolic activation (CCA) or CCR. If a *cre* box is in the promoter region, the binding of either of these complexes leads to CCR by interfering with binding of the transcription machinery (Asai et al., 2000). If a *cre* box is within the gene, the binding causes a transcriptional roadblock by blocking transcription elongation (Fujita, 2009; Puri-Taneja et al., 2006). Additionally, in many *Bacillus* spp., glucose exerts a form of inducer-exclusion by competing with xylose for interaction with the xylose repressor (XylR), and inhibits the induction of transcription of the xylose utilization operon (Jones et al., 2002). However, these mechanisms are only part of the CCR puzzle, and more studies are needed to fill the gaps (Hueck and Hillen, 1995). For example, glucose exerts additional XylR-dependent repression in *B. subtilis* and *B. megaterium*, but not in *B. licheniformis* (Dahl et al., 1995; Pogrebnyakov et al., 2017). Although *Parageobacillus* spp. have a close evolutionary relationship with *Bacillus* spp.(Hussein et al., 2015), their thermophilic nature might have resulted in a different sugar utilization pattern and a different CCR machinery.

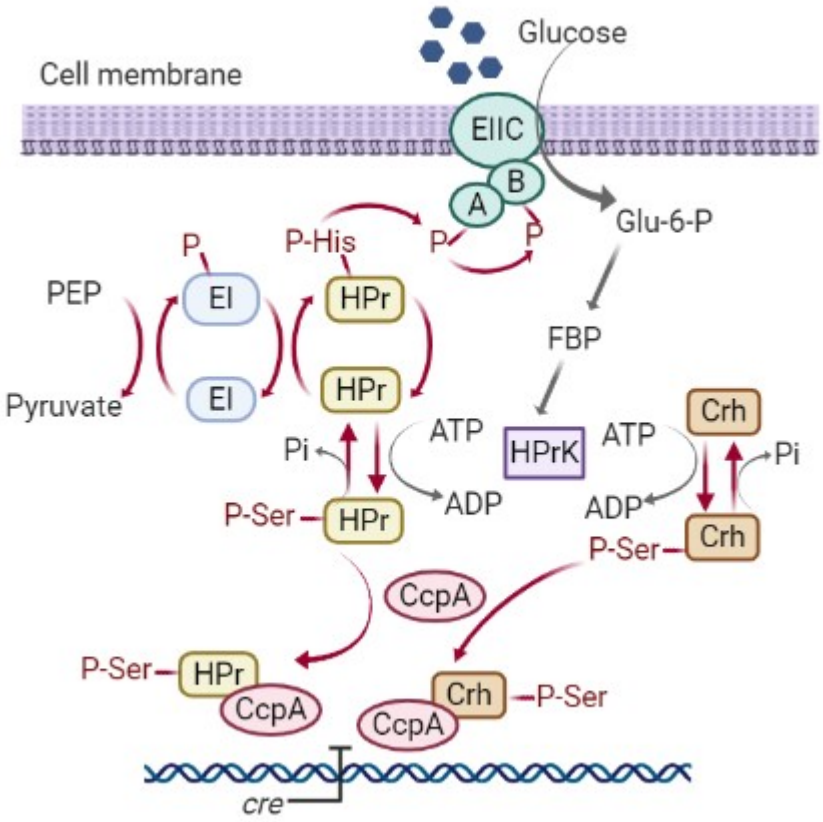

Figure 1: Signal transduction pathway of carbon catabolite repression (CCR) in Gram-positive bacteria Fujita (2009); Görke and Stülke (2008). HPr: phosphocarrier protein; Crh: catabolite repression HPr; CcpA: carbon catabolite protein A; HPrK: HPr kinase; EI: Enzyme I; EII: Enzyme II; PEP: phosphoenolpyruvate; Glu-6-P: glucose-6-phosphate; FBP: fructose-1,6-bisphosphate; *cre*: catabolite-response element; ATP, adenosine triphosphate; ADP, adenosine diphosphate.

The aim of this study is to investigate CCR in *P. thermoglucosidasius* on physiological and molecular levels. For physiological studies, reductive-oxidative (redox) potentials were defined here for the growth of *P. thermoglucosidasius* DSM 2542 under oxygen-limited, micro-aerobic and fermentative conditions. When the oxygen demand of a culture exceeds the oxygen supply, the redox potential becomes a useful parameter to monitor and control the oxygen availability. Redox potentials not only reflect the outcome of reduction-oxidation reactions in the external solution, but also reflect the balance of the reducing equivalents within the cells, which are relevant to central metabolism (Liu et al., 2011). Previously, redox potential measurements have been applied to metabolic analysis. For example, in *P. thermoglucosidasius* NCIMB 11955, many proteins are expressed differentially depending on the oxygen availability, which led to changes in cell behaviour at different redox potentials (Loftie-Eaton et al., 2013). ^{13}C-Based flux analysis in *P. thermoglucosidasius* M10EXG indicated that the oxygen concentration had a significant impact on metabolic fluxes through the central pathways (including glycolysis, pentose phosphate pathway, tricarboxylic acid (TCA) cycle and anaplerotic pathways) (Tang et al., 2009). Therefore, controlling the redox potential in a bioreactor should allow for more defined conditions for physiological study.

2 Materials and methods

2.1 Bacterial strains used in this study

Table 1: Bacterial strains used in this study

Strain	Description	Source
P. thermoglucosidasius DSM 2542	Wild type strain	DSMZ, Braunschweig
E. coli DH5α	Cloning strain, F-, *φ80lacZΔM15 Δ(lacZYA-argF)* U169 *recA1 endA1 hsdR17 (rK– mK+) phoA supE44 λ-thi–1 gyrA96 relA1*	David Leak Lab, University of Bath (Grant et al., 1990)
E. coli S17-1	Tp^R Sm^R *recA, thi, pro, hsdR-M*+RP4:2-Tc:Mu:Km Tn7 λpir	David Leak Lab, University of Bath (Stabb and Ruby, 2002)

2.2 Standard reagents and bacterial growth media

All reagents were purchased from Sigma Aldrich (Dorset, UK) or Fisher Scientific (Loughborough, UK). Ingredients of each medium are listed in the following table.

Table 2: Bacterial growth medium.

Media	Ingredients per litre of media
LB	Tryptone 10 g, Yeast extract 5 g, NaCl 5 g, adjusted to pH 7.0 with NaOH
SOC	Tryptone 20 g, Yeast extract 5 g, NaCl 0.5 g, KCl 0.186 g, $MgCl_2$ 0.952 g, glucose 3.603 g, adjusted to pH7 with NaOH
2TY	Tryptone 16 g, Yeast extract 10 g, NaCl 5 g, adjusted to pH 7.0 with NaOH
ASM	1.68 g citric acid, 1.23 g $MgSO_4$, 1.74 g K_2SO_4, 3.12 g NaH_2PO_4, 0.09 g $CaCl_2$, 3.3 g $(NH_4)_2SO_4$, 0.4 mg Na_2MoO_4, 3.6mg Thiamine, 1.46 mg biotin, 5 mL Trace element solution, buffered by adding 40 mL Bis-Tris, 40 mL HEPES and 40 mL MOPS solution (stock concentration 1M and at pH 7.0), final pH adjusted to 7.0 with KOH, filter sterilized. Trace element solution (1L): 1.44 g $ZnSO_4.7H_2O$, 0.56 g $CoSO_4.6H_2O$, 0.25 g $CuSO_4.5H_2O$, 5.56 g $FeSO_4.6H_2O$, 0.89 g $NiSO_4.6H_2O$, 1.69 g $MnSO_4$, 0.08 g H_3BO_3, 5mL 12M H_2SO_4
TGP	17 g tryptone, 3 g soy peptone, 5 g NaCl, 2.5 g K_2HPO_4, 8 mL glycerol and 8 mL sodium pyruvate (0.5 g/mL dissolved in deionised water) sterilized by filtration were added after autoclaving. SOC medium was used for the recovery of *E.coli* after transformation with the heat-shock method.

Ingredients were dissolved in deionised water and autoclaved (121°C and 15 psi for 20 min), unless otherwise stated. To make agar plates, 15 g agar was added to 1 L liquid medium before autoclaving, and if appropriate, kanamycin sulphate was added post-autoclaving after the medium had been cooled down to about 55°C.

2.3 Correlation of cell dry weight and OD_{600}

Optical density was correlated to biomass concentration for *P. thermoglucosidasius* DSM 2542 for growth study. Biomass concentration to OD_{600} (optical density of a sample measured at a wavelength of 600 nm) correlation for DSM 2542 was determined using biomass obtained from 50 mL shake flask cultures in ASM medium supplemented with 1% (w/v) glucose and 1% (w/v) xylose. Cells were harvested by centrifugation at 3200×g for 10 min and re-suspended in 15 mL ASM medium. A series of dilutions was prepared in triplicate. 10 mL of each dilution was transferred into pre-dried, pre-weighed fresh tubes and centrifuged at 3200×g for 10 min. Supernatant was removed and tubes containing the biomass were dried at 80°C for 24 h, then weighed on a semi-microbalance with accuracy to 0.01 mg (Ohaus Pioneer PX125D, SLS, Nottingham, UK). Tubes were dried and weighed again to ensure consistency, and the average weight of each dilution was used for calculation. The correlation curve is provided in Fig.A.1. Biomass to OD_{600} correlation for DSM 2542 was 0.42 g/L cell dry weight per unit OD_{600}.

2.4 Bench-top bioreactor operation

Batch growth of *P. thermoglucosidasius* was carried out in 2 L (working volume 1.5 L) bioreactor vessels equipped with Biostat B Plus conrollers (Sartorius, Germany) at 60°C. Cells were grown in ASM medium containing 1% (w/v) glucose and 1% (w/v) xylose (pH 7.0). pH/Rx probes (EASYFERM PLUS VP pH/Rx 255, Hamilton, Switzerland) and dissolved oxygen sensors (OXYFERM VP, Hamilton, Switzerland) were used to monitor the pH, redox potential and oxygen saturation in real time. Agitation was controlled by dual Rushton turbine impellers, and air was introduced via a sparger beneath the bottom impeller. 5 M KOH, 5 M H_3PO_4 and antifoam 204 (Sigma, Dorset, UK) were automatically injected if required (Hills, 2015). A starter culture was grown in 15 mL TGP medium for 4 to 5 h until the OD_{600} reached 2.5∼3.0. Then, 1 mL of the starter culture was inoculated into 50 mL ASM medium in a 250 mL baffled Erlenmeyer flask and grown at 60°C. All 50 mL was inoculated into the bioreactor when the cells reached an OD_{600} of 1.5∼2.0 in 12 to 14 hours.

A fermentative condition was defined (section 3.2) and controlled by the redox potential during growth. Cultures were firstly grown under aerobic conditions [agitation 600 rpm, air 1 vvm (volume gas per volume liquid per minute)] until they reached an OD_{600} of about 0.2. After that, agitation and air inflow were reduced and automatically controlled by a cascade system to ensure that the redox potential was between -270 mV and -290 mV. Samples were taken at regular intervals by pulling a vacuum with a syringe for transfer into tubes, and the corresponding redox potentials were recorded. Sugars and fermentation products in the samples were analysed by HPLC. Growth rate, substrate coefficient and sugar consumption rates were determined using the slope between the lag phase and stationary phase.

2.5 HPLC analysis

Residual sugars and metabolic products arising during cell growth were quantified using an Agilent 1200 Series HPLC system (Agilent Technologies, Santa Clara, USA). Samples were sterile-filtered (Phenex-NY 15mm Syringe Filters 0.2 μm, Phenomenex, Torrance, USA) to obtain a cell-free supernatant. Sugars and ethanol were analysed by an Agilent 1200 Series G1362A Infinity Refractive Index Detector (RID), while organic acids were analysed by an Agilent 1200 Series G1314B Variable Wavelength Detector at a wavelength of 215 nm (Al-Hinai et al., 2015). A Phenomenex Rezex RHM Monosaccharide H column (300 mm × 7.8 mm,

Phenomenex Inc, Torrance, CA) maintained at 65°C was used for analyte separation, with 5 mM H_2SO_4 as the mobile phase (0.6 mL/min, 25 min)(Raita et al., 2016). Peak area quantification was performed using Agilent ChemStation software. Standard curves were constructed to determine the concentration of each compound according to ChemStation Manual (G2070-91126).

2.6 Conjugation

Plasmid pG1AK-oriT-pheB was constructed by ligating the previously made plasmid pG1AK-pheB (Reeve et al., 2016) with an origin of transfer (oriT) and a *traJ* gene encoding TraJ, an oriT recognising protein (Ortenzi, unpublished). Chemically competent *E.coli* S17-1 was prepared and transformed with the plasmid pG1AK-oriT-pheB using a heat-shock method (Chang et al., 2017), and presence of the plasmid was confirmed by colony PCR. The S17-1 cells containing the desired plasmid were inoculated into 10 mL LB medium containing 50 μg/mL kanamycin and cultured overnight at 37°C. The next morning, these cells were initially chilled on ice. Simultaneously, *P. thermoglucosidasius* DSM 2542 was grown overnight in 10 mL TGP or 2TY medium at 60°C. In the morning, this culture was diluted in 10 mL fresh 2TY medium to about OD_{600} 0.1 and grown as before until the OD_{600} reached about 1.0. Then, the S17-1 was centrifuged at 3,220×g (25°C, 10 min). Supernatant was removed and the cells were re-suspended in 10 mL of LB medium by gentle pipetting. Next, 1 mL of the S17-1 suspension was mixed with 9 mL of the DSM 2542 culture and centrifuged at 3,220×g (25°C, 2 min). After discarding the supernatant, the cells were re-suspended with the remaining liquid by gentle pipetting, and transferred to a single spot on an LB plate supplemented with 10mM $MgCl_2$. The plate was then incubated overnight at 37°C facing upwards. The next day, the cells were scraped from the plate and re-suspended in 1 mL of 2TY. The cell suspension was serially diluted (10^{-1}, 10^{-3}, 10^{-5}, 10^{-7}) and 100 μL of each dilution was spread onto a 2TY agar plate containing 12.5 μg/mL kanamycin. Plates were incubated at 52°C overnight to isolate successful transconjugants (Macklyne, 2017).

2.7 Preparation of RNA from *P. thermoglucosidasius* cultures

DSM 2542 seed culture was grown at 60°C in ASM medium supplemented with 1% (w/v) glucose, 1% (w/v) xylose or a mixture of 1% (w/v) glucose and 1% xylose. 1 mL of the seed culture was inoculated into 25 mL of fresh ASM medium supplemented with corresponding sugars in 50 mL centrifuge tubes. Cells grown 60°C to an OD_{600} of 1.5∼1.8 were combined with 30 mL RNAlater (Sigma-Aldrich, Dorset, UK), vortexed for 5 sec, then incubated for 5 min at room temperature. Cells were then harvested by centrifugation for 10 min at 3,220×g at 4°C and, after discarding the supernatant, the tubes were dried by inverting on paper towels and then stored at -80°C. To isolate RNA, cell pellets were defrosted and re-suspended in 250 μL of lysis bufer [30 mM Tris–HCl, 1 mM EDTA, pH 8.0, 15 mg/ml lysozyme (Sigma-Aldrich, Dorset, UK), 20 μL Proteinase K (600 U/mL, Thermo Scientific, Paisley, UK)] and incubated for 10 min at room temperature, followed by vigorously vortexing for 10 sec every 2 min. RNA isolation and purification were performed using the RNAeasy Mini Kit (Qiagen, Manchester, UK) following the manufacturer's instructions. The RNA concentration and purity was measured with a NanoVue Plus Spectrophotometer (Biochrom, Cambridge, UK) (Bacon et al., 2017).

2.8 qRT-PCR analysis of xylose isomerase mRNA expression

Table 3: Primers used for qRT-PCR.

Oligonucleotide name	Sequence
xylA Fw	ttaggatgggatacggacga
xylA Rw	ggcgatatgggcatagaaca
rpoB Fw	ctcttggctttggctctgac
rpoB Rw	gacgcaaacgctcgtaaatc
recN Fw	cgttgtcggtttcgtttgac
recN Rw	gcccttctatttccgccttt
oopF Fw	gtctagtgccgatagatggttctc
oopF Rw	agctcgctgtgtgtccattc

cDNA was generated using a High-Capacity cDNA Reverse Transcription Kit (Applied Biosystems, California, USA). A total of 1 μg RNA was used per reaction, and RNase inhibitor was added according to manufacture's instructions. The cDNA concentration and purity was measured with a NanoVue Plus Spectrophotometer (Biochrom, Cambridge, UK) (Bacon et al., 2017; Bartosiak-Jentys, 2011).

Th genes encoding the DNA repair protein (*recN*) and the β subunit of RNA polymerase (*rpoB*) were used as reference genes as described previously (Bacon et al., 2017). *OopF*, encoding a peptide ABC transporter ATP-binding protein, acted as an endogenous control. To detect the expression level of the target genes and the reference genes, primers were designed with Primer3Plus software based on the criteria defined by OpenWetWare (OpenWetWare, 2013), and the primer efficiency was tested. LuminoCt SYBR Green qPCR Readymix (Sigma-Aldrich, Dorset, UK) was used for qPCR reactions following the manufacturer's instructions. The qPCR reaction was initiated by heating up to 95°C for 20 sec, followed by 40 cycles of denaturation (95°C, 5 sec), annealing and extension (60°C, 30 sec). At the end, a melt curve analysis was performed by raising the temperature from 55°C to 95°C at 0.2°C per 2 sec (Bacon et al., 2017).

2.9 Preparation of clarified cell extracts

Cells were harvested by centrifugation at 3200×g (4°C, 10 min) when they reached an OD_{600} 1.5∼1.8. The supernatant was removed and the cell pellets were washed in 20 mL 50 mM sodium phosphate buffer (pH 7.2) by pipetting. Then, the cells were pelleted by centrifugation at 3200×g (4°C, 10 min), and re-suspended in 1 mL 50 mM sodium phosphate buffer (pH 7.2) containing Pierce EDTA-free protease inhibitor (Thermo Scientific, Paisley, UK) (Bartosiak-Jentys et al., 2012). Cells were disrupted by sonication (Soniprep 150 Ultrasonic Disintegrator, MSE Crowley, London, UK) at 14 microns of probe amplitude on ice (3×20 sec with a 30 sec interval between each burst). Cell lysate was transferred to a 1.5 mL micro-centrifuge tube, and centrifuged at 11,400×g at 4°C for 15 min to remove insoluble debris (Hills, 2015). The supernatant was transferred to a fresh 1.5 mL micro-centrifuge tube. The protein concentration was determined in 96 microtiter plates (Griener BioOne, Stonehouse, UK) using the Bradford Protein Assay Kit (Bio-Rad, Hemel Hempstead, UK) following the manufacturer's instructions.

2.10 Quantitative assay for catechol 2,3-dioxygenase activity with *pheB* as a reporter gene

Catechol 2,3-dioxygenase catalyses the cleavage of catechol to form 2- hydroxymuconate semialdehyde (HMSA) (Ishida et al., 2002), which can be detected at λ=375nm, making it useful for continuous assays to record expression levels. A saturating substrate concentration of 0.33 mM catechol was used for the experiments (Bartosiak-Jentys, 2011). The reactions were done in 1 mL quartz cuvettes; 600 μL of 50 mM sodium phosphate buffer (pH 7.2) and 33 μL of 10 mM catechol were mixed in the cuvette and pre-incubated at 55°C for 2 min. The reaction was initiated by adding 367 μL clarified cell extract, with absorbance readings measured continuously over 10 min in a Varian Cary 50 UV-Vis Spectrophotometer (Varian, Agilent Technologies, Santa Clara, USA). As the reaction follows a 1:1 stoichiometry, the concentration of accumulated HMSA (ϵ= 33 mM/cm at λ=375 nm) should be equivalent to that of the oxidized catechol (Nozaki et al., 1970). The rate of change in absorption at λ=375 nm per minute (ΔA) was calculated from the gradient of the absorbance readings during the accumulation of HMSA (Bartosiak-Jentys, 2011). The rate of change in HMSA concentration per minute (Δc) can be determined using the Beer-Lambert law equation (path length l =1cm): $\Delta c = \frac{\Delta A}{\epsilon \cdot l}$

Δc for HSMA has the unit of mM/min, and 1mM/min is the equivalent of 1 μmol/min in a 1 mL cuvette (Bartosiak-Jentys, 2011). This was divided by the amount of protein (mg) added to the cuvette, giving the catechol 2,3-dioxygenase activity in μmol/min/mg or nmol/min/mg (Bartosiak-Jentys, 2011).

3 Results

3.1 Physiology of CCR in *P.thermoglucosidasius* DSM 2542 in shaking flasks

A preliminary study of CCR in DSM 2542 was carried out in 250 mL silicone sponge sealed baffled Erlenmeyer flasks in an Innova 44 shaking incubator (New Brunswick, UK) at 60°C and 250 rpm. The flasks contained 50 mL ASM medium supplemented with 0.5% (w/v) glucose and 0.5% (w/v) xylose. According to the HPLC profiles, acetate was produced as a metabolic product, while production of the fermentation products, lactate, formate and ethanol was not observed (data not shown). Previous studies suggested that acetate could be produced under respiratory growth (Vemuri et al., 2006), so the culture conditions here were considered as aerobic. As shown in Fig.2, DSM 2542 prioritized the utilization of glucose, suggesting that DSM 2542 is subject to CCR under aerobic conditions. However, information provided by the shake flask cultures was limited because the dissolved oxygen and pH could not be monitored and controlled in real time (Vemuri et al., 2006). Hence, it was decided to perform the oxygen-limited growth studies of DSM 2542 in the bioreactor, where the dissolved oxygen and pH could be better controlled.

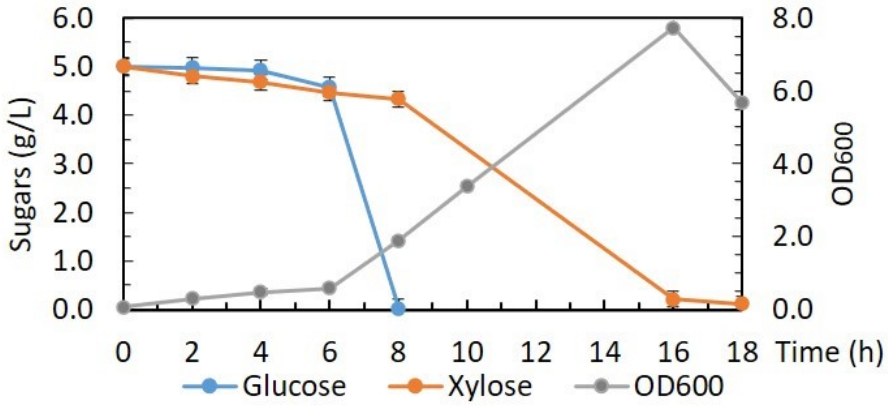

Figure 2: Growth curve and sugar consumption of *P. thermoglucosidasius* DSM 2542 in shaking flasks at 60°C in ASM supplemented with 0.5% (w/v) glucose and 0.5% (w/v) xylose.

3.2 Determination of operating conditions for micro-aerobic and fermentative growth using redox potentials.

Initially the growth rates and metabolic products of *P. thermoglucosidasius* DSM 2542 in the bioreactor at different redox potentials at 60°C were compared. Aerobic status was achieved by setting the aeration to 1 vvm and controlling the agitation based on the redox potential. In agreement with previous data (Loftie-Eaton et al., 2013), when the redox potential was positive, no significant fermentation products (e.g. lactate) were observed in the HPLC profile (data not shown). When aeration and agitation reduced, negative redox potentials indicated oxygen supply became limited. A micro-aerobic condition was achieved by reducing the aeration rate at least five-fold. When the redox potential was negative and greater than -200 mV, acetate was the main metabolic product. When the redox potential was controlled in a range of -220 mV -240 mV, lactate was the main fermentation product, with little formate or ethanol produced. When the redox was between -270 mV and -290 mV, formate and ethanol were also produced in addition to lactate. Although lactate is typically classified as a fermentation products in the sense that it is a reduced carbon compound produced to allow re-oxidation of NADH, it could be excreted as an over-flow metabolite when the rate of glucose consumption is greater than the capacity to oxidise NADH to NAD^+ via the respiratory chain(Campbell et al., 2018), with the production of ethanol and formate via the pyruvate formate lyase pathway being the main fermentation pathway. The growth rate was the fastest with redox > -200 mV), slower when the redox potential was in the range -220 mV to -240 mV, and the slowest when it was in the range -270 mV to -290 mV (Fig.3A). Consistent with the gradual switch from respiratory to fermentative energy generation the cells consumed increasing amounts of glucose per gram of cells as the redox decreased from > -200 mV to -270 mV$\sim$ -290 mV, but this pattern was as obvious in xylose consumption (Fig.3B). For this study we defined growth at a redox potential of -270 mV$\sim$ -290 mV as fully fermentative, where DSM 2542 could enter full mixed acid fermentation while aeration and agitation were limited.

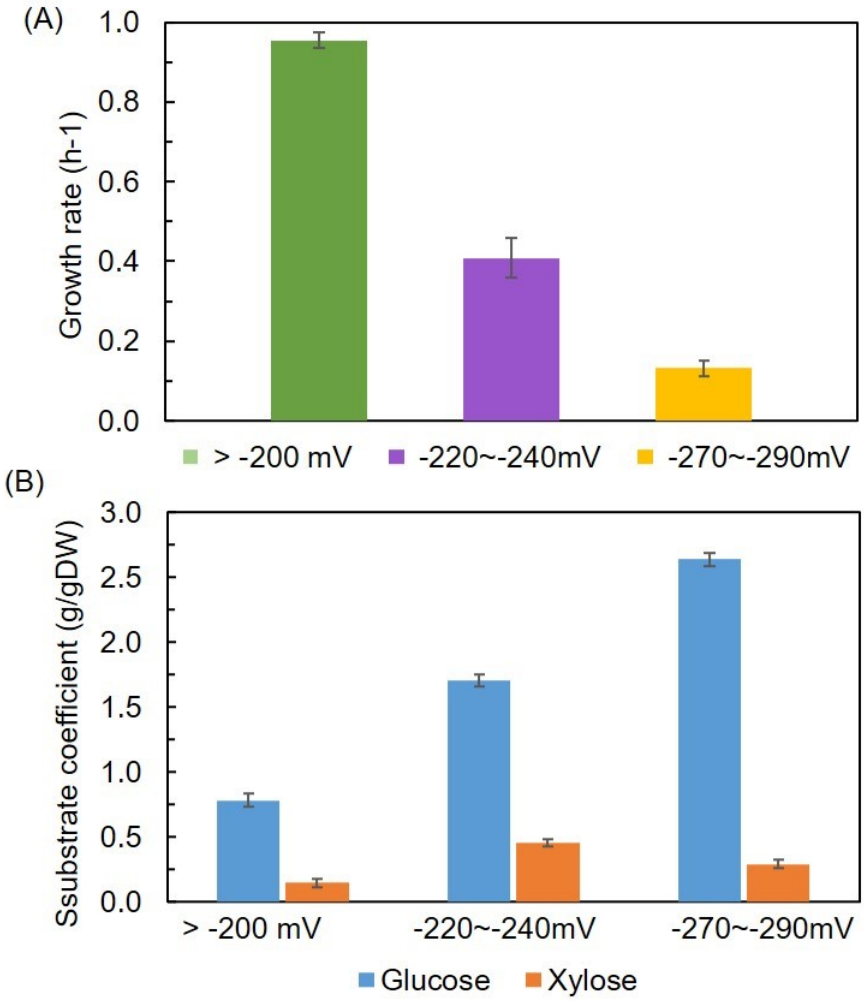

Figure 3: (A) Growth rate and (B) substrate coefficient (g/gDW, gram per gram of dry weight of cell mass) of *P. thermoglucosidasius* DSM 2542 at 60°C under different redox conditions in ASM supplemented with 1% (w/v) glucose and 1% (w/v) xylose. Error bars are standard deviation of three technical replicates for each condition.

3.3 Physiology of CCR in *P.thermoglucosidasius* DSM 2542 under fermentative conditions

Under fermentative conditions, when glucose or xylose was the sole carbon source, DSM 2542 could utilize either sugar with a similar consumption rate. The sugar consumption rate was 0.22 g/gDW/h (gram per gram of cell dry weight per hour) on glucose as the sole carbohydrate, and 0.19 g/gDW/h on xylose alone (Fig.4A). In a medium containing both glucose and xylose, the rate of glucose consumption (0.24 g/gDW/h) was similar to that of glucose alone, while and the rate of xylose consumption (0.03 g/gDW/h) suggested that CCR was also occurring under fermentative conditions (Fig.4B). However, unlike the typical model of CCR where glucose metabolism completely inhibits xylose metabolism, the CCR in DSM 2542 under fermentative conditions seemed more relaxed. A small amount of xylose was consumed together with the glucose, although much more slowly than when xylose was the only carbon source. After all the glucose was consumed cell growth virtually stopped, even though the cells continued to

metabolise xylose, suggesting that the energy produced was largely being used for maintenance purposes (Fig.4C).

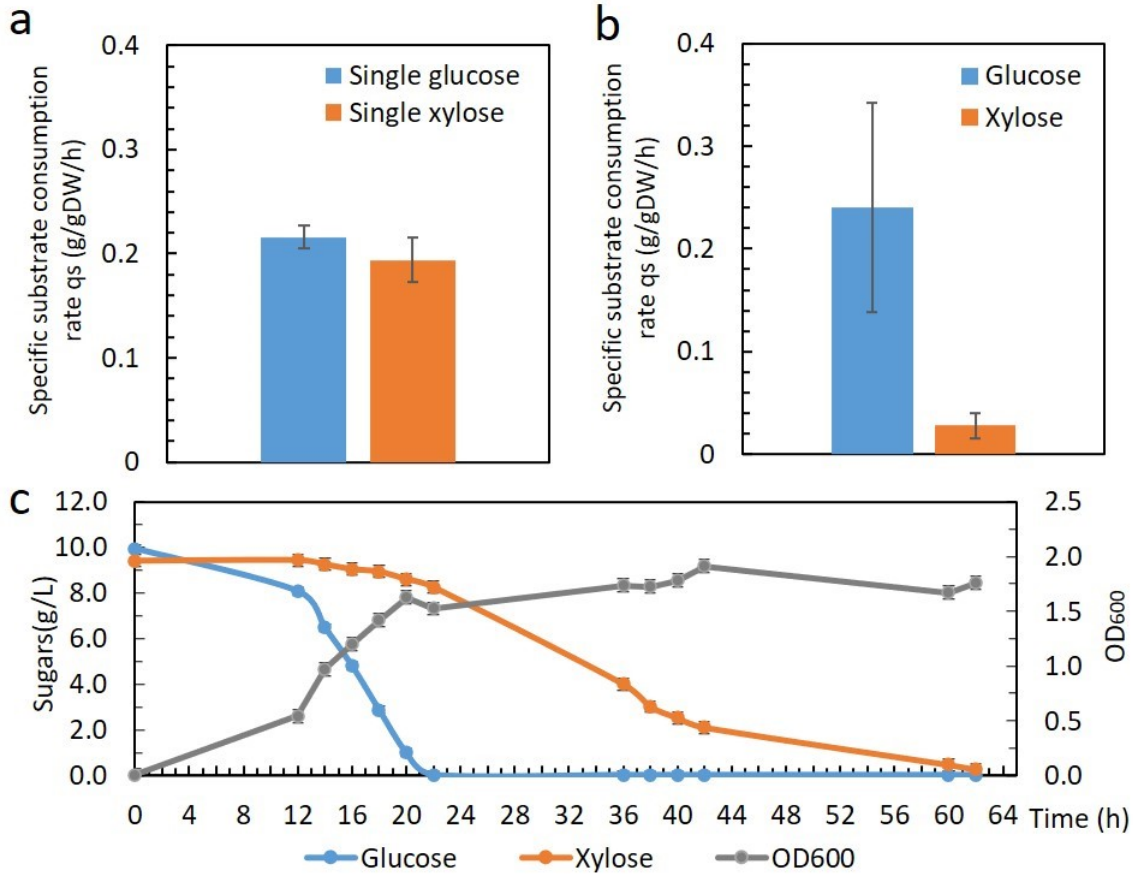

Figure 4: Fermentation profile and sugar consumption of *P. thermoglucosidasius* DSM 2542 in ASM supplemented with different sugars under fermentative conditions in bioreactors. Error bars are ± standard deviation of two biological repeats. (A) Sugar consumption rate (g/gDW/h, gram per gram of dry weight of cell mass per hour) in ASM supplemented with 1% (w/v) glucose or 1% (w/v) xylose. (B) Sugar consumption rate (g/gDW/h) in ASM supplemented with 1% (w/v) glucose and 1% (w/v) xylose. (C) Fermentation profile of DSM 2542 in ASM supplemented with 1% (w/v) glucose and 1% (w/v) xylose.

3.4 qRT-PCR analysis of *xylA* mRNA expression under oxygen-limited conditions

CCR, like many bacterial regulatory processes, typically operates through the control of transcription. Given the evidence for operation of CCR under fermentative conditions it was important to assess whether CCR in *P. thermoglucosidasius* DSM 2542, also involves regulation of transcription during cell growth. Therefore, qRT-PCR was used to measure the rate of transcription of the xylose isomerase gene *xylA* in cultures grown in ASM medium supplemented with either 1% (w/v) glucose, 1% (w/v) xylose or a mixture of 1% (w/v) glucose and 1% (w/v) xylose. Oxygen-limited conditions were achieved by growing 25 mL cultures in 50 mL sterilized conical tubes, allowing for an initial aerobic growth until the oxygen demand exceeded supply (Bartosiak-Jentys, 2011). A qPCR reaction was set up as described in section 2.8 using 5 ng cDNA with primer pairs (Table 3) targeting either the *xylA* or the reference genes (*recN* and *rpoB*) (Cuebas et al., 2011; Mohkam et al., 2016). The average C(t) value was calculated for each condition and primer pair, and relative expression levels of the *xylA* under different sugar

conditions were determined using the Pfaffl equation (Bacon et al., 2017).

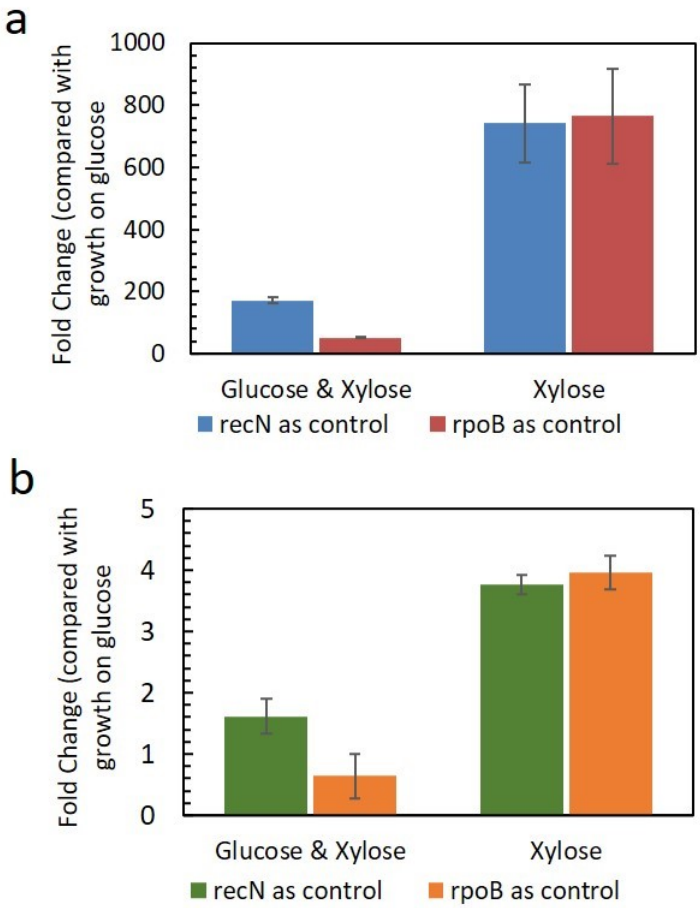

Figure 5: Ratio of (A) *xylA* and (B) *oopF* expression under mixed glucose and xylose: glucose conditions, or xylose: glucose conditions. *recN* and *rpoB* were used as the reference genes. *P. thermoglucosidasius* DSM 2542 was grown in in ASM supplemented with 1% (w/v) glucose, 1% (w/v) xylose, or mixed 1% (w/v) glucose and 1% (w/v) xylose under oxygen-limited conditions. cDNA from each condition was tested with each primer set in triplicate. The average C(t) values for each condition and primer set were used to determine the ratio of gene expression using the Pfaffl equation (Bacon et al., 2017). Error bars are ± standard deviation of two biological repeats.

With either of the reference genes, expression of the *xylA* was about 750 fold higher when DSM 2542 was grown on xylose compared with when it was grown on glucose (Fig.5A). Consistent with the partial repression of xylose utilization observed during fermentative growth (section 3.3), the *xylA* was up-regulated when DSM 2542 was grown on a mixture of glucose and xylose compared with when it was grown on glucose alone (about 170 fold higher when *recN* was the reference gene, and about 50 fold higher when *rpoB* was the reference gene). The difference in ratios suggests that expression of the reference genes may vary depending on growth conditions (Radonić et al., 2004). Although expression of housekeeping genes should ideally not change much between tested conditions, in *E. coli* the expression of the *rpoB* gene encoding for the β subunit of RNA polymerase is known to vary with growth rate and exhibits elements of transcriptional and translational control. Consequently, when *rpoB* was the reference gene in mixed sugars conditions, increased expression would mean that the fold change was smaller than when using *recN*. The endogenous control *oopF* exhibit a very small variation when expressed under different sugar conditions compared to the *xylA* (Fig.5B). As expected, it seems that the expression of *oopF* might not be significantly affected by different sugars.

However, in *B. subtilis*, expression of the peptide ABC transporter operon increased during the exponential phase, reaching a maximum value at the stationary phase, and decreased during the death phase (Koide et al., 1999). Because of the difference in growth rate on glucose and xylose, we might expect some variation in expression of *oopF* between growth on glucose and xylose. In summary, the partial induction of *xylA* during growth on glucose plus xylose confirms that, while some catabolite repression is occurring, it is relatively relaxed in *P. thermoglucosidasius* DSM 2542 compared with *E. coli* and many other organisms (Chen et al., 2018; Li et al., 2016; Zhang et al., 2016).

3.5 Using *pheB* as a reporter gene to study CCR in *P. thermoglucosidasius* DSM 2542 under oxygen-limited conditions

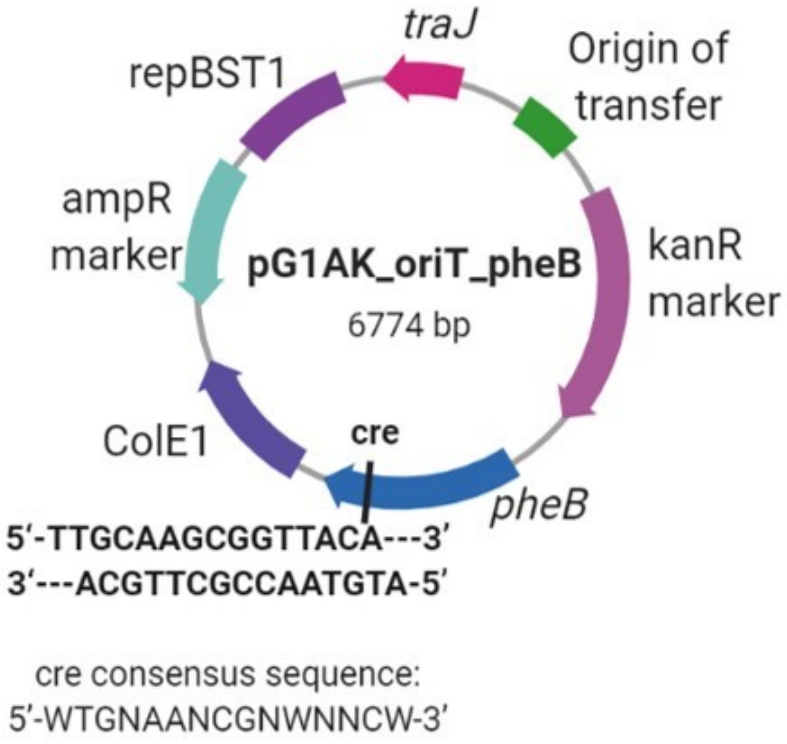

Figure 6: Plasmid pG1AK-oriT-pheB used in this study. The plasmid contains a reporter gene system based on a *pheB* gene behind a constitutive pRplsWT promoter. The *pheB* gene contains a pair of palindromic *cre* sites towards the end of the gene.

To further study how CCR affects gene expression in *P.thermoglucosidasius* DSM 2542, a reporter gene system based on the *pheB* gene (GenBank accession no. DQ146476.2) was recruited (Bartosiak-Jentys et al., 2012). Sequence analysis of the *pheB* gene, which encodes catechol 2,3-dioxygenase, showed that it contains a previously unreported pair of palindromic *cre* sites towards the 3′ end of the gene (Fig.6). This gives it specific value as a catabolite sensitive reporter gene in its own right, without fusion to other genetic elements. A DSM 2542 transconjugant containing pG1AK-oriT-pheB was inoculated into 15 mL TGP medium supplemented

with 12.5 μg/mL kanamycin and grown for 6 to 8 hours at 52 °C until OD_{600} reached 1.5∼1.8. To obtain oxgen-limited growth, 500 μL of the above culture was inoculated into 25 mL ASM in a 50 mL sterilized conical tube, supplemented with 12.5 μg/mL kanamycin and 1%(w/v) glucose, or 1% (w/v) xylose, or 1%(w/v) glucose and 1% (w/v) xylose. The next morning, the cells were harvested, and cell extracts were prepared for catechol 2,3-dioxygenase enzyme assays as described (section 2.9). Consistent with the transcriptional profile, the results showed that expression of *pheB* was higher during growth on xylose than on glucose, and strongly repressed when grown in a combination of glucose and xylose (Fig.7A). This is consistent with glucose acting as a strong catabolic repressor via the interaction of signalling molecules with the *cre* locus. Interestingly, the "relaxed" model of CCR was not observed here, probably due to the fact that the pair of *cre* loci in the *pheB* gene form a good palindrome when read with the previously-revealed *cre* consensus sequence 5′-WTGNAANCGNWNNCW-3′ (Bartosiak-Jentys et al., 2013). This might be relevant to the stringency of the *cre* sequences which will be discussed later (Inácio et al., 2003). Similar results were obtained with arabinose in place of xylose but, intriguingly, the catechol 2,3-dioxygenase activity was much higher during growth on arabinose alone than on xylose alone or on mixed xylose and arabinose (Fig.7B). This suggested that xylose metabolism might also be exerting a degree of CCR and this idea was supported by the fact that, when grown on a mixture of xylose and arabinose the catechol 2,3-dioxygenase activity was close to the lower level observed on xylose alone. It appears that glucose, xylose and arabinose form a hierarchical order in their ability to exert CCR through the *cre*. This suggests that this *cre* containing reporter gene could be a valuable tool for investigating the intricacies of CCR in *Parageobacillus* and *Geobacillus* spp., and possibly also in *Bacillus* spp.

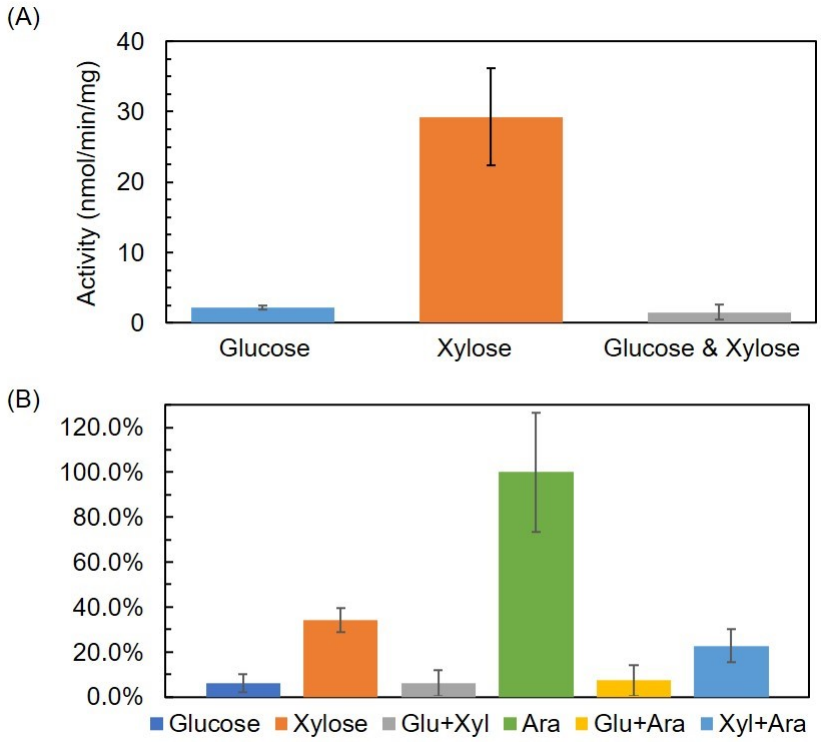

Figure 7: (A) Catechol 2,3-dioxygenase activity under single glucose, single xylose and mixed sugars conditions. (B) Ratio of catechol 2,3-dioxygenase activity under different sugar conditions in comparison with arabinose conditions. Error bars are ± standard deviation of two biological repeats.

3.6 Bioinformatic analysis of xylose utilization (*xyl*) operons

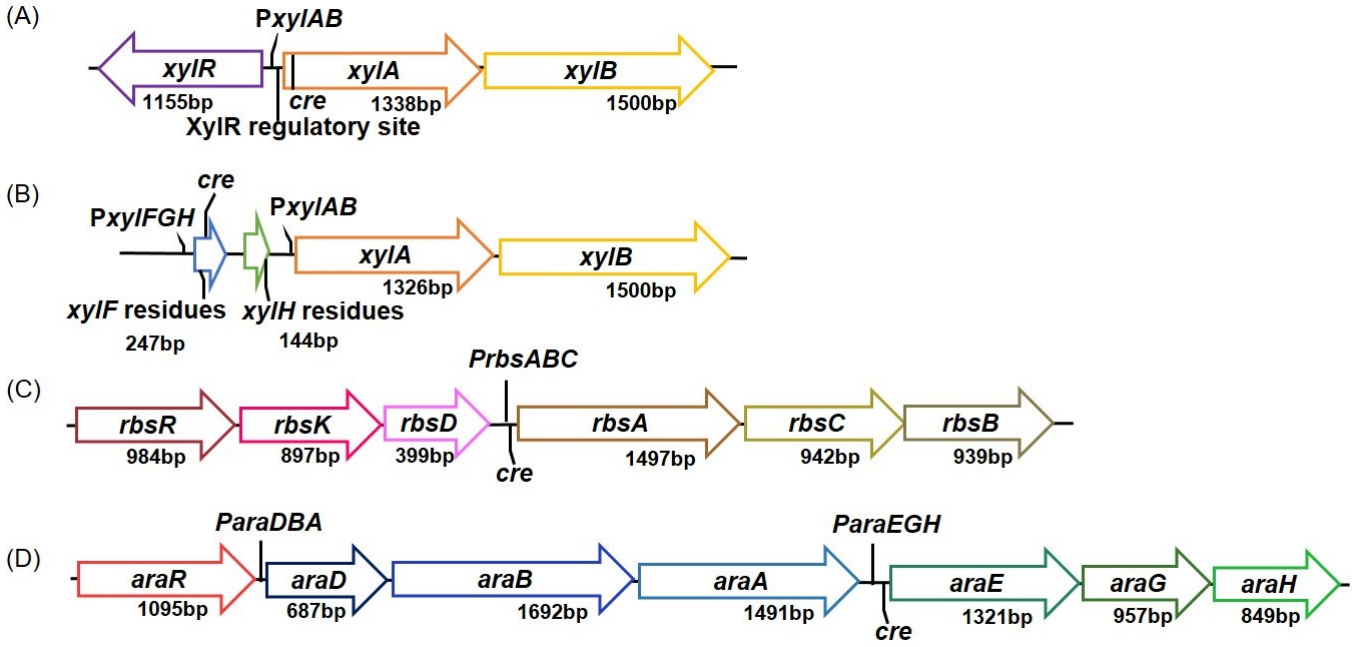

Figure 8: Schematic organization of the xylose uptake and utilization genes in (A) *B. subtilis* 168 and (B) *P. thermoglucosidasius* DSM 2542, as well as the (C) ribose and (D) arabinose uptake and utilization genes in *P. thermoglucosidasius* DSM 2542.

The presence of genes encoding CcpA, Hpr and Crh, together with the presence of *cre* boxes in both *B. subtilis* and *P. thermoglucosidasius* suggests that the mechanism of CCR might be similar in these organisms. However, the genetic organization of the *xyl* operon appears to be different in these two species. In *B. subtilis*, the *xyl* operon consists of *xylA* encoding xylose isomerase, *xylB* encoding xylulose kinase, and the divergently transcribed regulator gene *xylR*, with a *cre* element located within the coding region at the 5′ end of the *xylA* (Fig.8A) (Dahl and Hillen, 1995). In the absence of xylose, XylR binds to the regulatory site 5′-GTTTGTTTAAACAACAAACTAAT-3′ upstream of the *xylAB* operon (Rodionov et al., 2001). Xylose interacts with XylR to induce the expression of the *xylAB* operon by depression, while glucose has a dual effect on inhibiting xylose utilization. On one hand, glucose competes with xylose for binding to XylR and imposes an anti-inducing effect on the *xyl* operon. On the other hand, it exerts CCR via the binding of the CcpA-HPr (Ser46-P) or CcpA-Crh (Ser46-P) complex to the *cre* sequence within the *xylA* gene (Conejo et al., 2010). However, orthologues of *xylR* were not found in the DSM 2542 genomic sequence when searched with the NCBI BlastX tool (Basic Local Alignment Search Tool) (Altschul et al., 1997), neither was there any apparent XylR regulatory site within or upstream of the *xylAB* operon according to sequence alignments (Benchling bioinformatics platform) (Fig.8B). Hence, it is likely that the *xylAB* operon in DSM 2542 is not subject to XylR regulation. Furthermore, unlike *B. subtilis*, there is no *cre* site within the *xylAB* operon in DSM 2542. Interestingly, upstream of the *xylA* promoter region are the remnants of *xylF* and *xylH* genes from which there appears to have been a large deletion, removing a large fraction of the 3′ end of the *xylF* gene and 5′ end of *xylH* (Fig.8B). To confirm that this was not a genome assembly error, the DNA sequence of this region was confirmed by whole genome sequencing (MicrobesNG, Birmingham, UK) and PCR fragment sequencing (Eurofins Genomics, Ebersberg, Germany). Although the *cre*-like

sequence located within the remaining *xylF* gene fragment upstream of the *xylA* gene might exert CCR due to effects on read-through to the *xylAB* operon, this repression is likely to be small as a *xylAB* operon has its own promoter. This suggests that DSM 2542 does not have a dedicated xylose transport system but, similar to *B. subtilis*, may be able to use other pentose transporters. Notably, while *P. thermoglucosidasius* DSM 2542 does not encode a *xylR*, its arabinose and ribose regulon have genes encoding their own repressor proteins, namely *araR* (AOT13_11450) and *rbsR* (AOT13_01820) respectively, and associated transport systems with *cre* sites (Fig.8C and D). Hence, xylose uptake might be subject to the regulatory control of AraR and RbsR and exploit a reduction in specificity of their transport systems.

4 Discussion

Contrary to suggestions that thermophiles are not subject to catabolite repression, a loosely controlled CCR has been shown to operate on xylose metabolism in *P. thermoglucosidasius* DSM 2542. From bioinformatic analysis alone it is evident that *Parageobacillus* and *Geobacillus* spp. encode the components of a typical Firmicute CCR system, although physiologically there are distinct differences from that operating in *B. subtilis* 168. The loose control could reflect the stringency of the *cre* sequences involved which may be an advantage if CCR is operating on expression of the transporter genes, rather than the dedicated metabolic functions. Previous studies on other Firmicutes have shown that the level of glucose repression on different catabolic genes varies considerably, due to a striking variation in the cre-like sequences (Warner and Lolkema, 2003b). These variations determine the affinity of CcpA for the *cre* site, and therefore affect the stringency of CCR (Inácio et al., 2003). In *P. thermoglucosidasius* NCIMB 11955 (which is virtually identical to DSM 2542), a consensus *cre* sequence 5′-WTGNAANCGNWNNCW-3′ has been identified (Bartosiak-Jentys et al., 2013). Using this consensus sequence, a pair of *cre* loci which form a good palindrome was fortuitously-revealed in the *pheB* gene, which has been shown in this study to be a versatile catabolite sensitive reporter gene. The *cre* box in *pheB* is near the 3′ end of the gene, so it presumably exerts CCR via the roadblocking mechanism. Although *cre* boxes are more typically close to the 5′ end of the gene (which would allow more efficient transcription termination), *cre* boxes near the 3′ end are not unknown (Fujita, 2009). *Cre* boxes are often partially palindromic, with a perfect palindrome giving very strong repression (Miwa et al., 2000). The highly palindromic *cre* box in the *pheB* gene (Fig.6) correlates with the observed tight control of CCR on *pheB* expression. Using *pheB* as a reporter gene, a hierarchical regulation of CCR exerted by glucose, arabinose and xylose was observed in *P. thermoglucosidasius* DSM 2542, with glucose being the strongest repressor, followed by xylose, then arabinose.

Furthermore, bioinformatic analysis was performed to investigate why the control of CCR on xylose utilization is not very stringent in *P. thermoglucosidasius* DSM 2542. Unlike the situation with *B. subtilis*, there is no *cre* within the *xylA* gene coding region in DSM 2542, nor in the promoter directly responsible for *xylA* transcription. Indeed, in the absence of a *xylR* and typical XylR binding site it is not clear how the expression of the *xylAB* operon is controlled, although it is clearly under some form of CCR. Potentially, catabolite control might occur indirectly via transcriptional regulation of genes responsible for xylose transport, but in the absence of a dedicated xylose transport system this must be operating through one or more of the other pentose transporters which are subject to the regulation of corresponding repressor proteins. The use of other pentose transporters for xylose transport has been described in organisms such as *B. subtilis*, which cannot grow rapidly in a minimal medium with xylose as the sole carbon source because it does not have a dedicated xylose transporter (Park et al.,

2012). In *B. subtilis* xylose is imported by an arabinose proton-symporter (AraE) (Krispin and Allmansberger, 1998). To investigate whether this may also be the case in DSM 2542, operons encoding a putative arabinose ABC transporter and a putative ribose ABC transporter were located. *Cre*-like sequences were found in the genes encoding both arabinose (AOT13_11475) and ribose (AOT13_01795) substrate-binding proteins, which are 5′-TTGAAAACGCAAAAA-3′ and 5′-TTGAAATCGATAACC-3′ respectively, indicating that these transporters are subject to CCR. These *cre*-like sequences differ by one base from the known consensus sequence 5′-WTGNAANCGNWNNCW-3′ (Kraus et al., 1994) probably because, during evolution, the *cre* sequence has been modified to ensure production of a functional protein (Miwa et al., 2000). As the efficiency of the *cre* decreases with a lower similarity to the consensus sequence, expression of these transporters might be subject to leaky control of CCR. Furthermore, these *cre*s are imperfect palindromes, so they might not give such strong repression as is the case with the highly palindromic *cre* in *pheB*.

Despite the incomplete resolution of the mechanism of induction and catabolite repression of the *xyl* operon(s), the evidence that *P. thermoglucosidasius* contains elements of a classical Firmicute CCR system suggests that strategies to alleviate CCR which have been applied to *Bacillus* spp. may also work in *Parageobacillus* spp. In particular these include site directed mutagenesis of the HPr and Crh proteins at their regulatory phosphorylation sites or inactivation of the associated kinase. If the operational *cre* sites can be established, then these might also be target for mutagenesis.

Authors contributions

Laboratory experiments were formulated by JL, DL and AB. Methodologies were designed by JL, DL and RvK. Experimental work was carried out by JL (90%) and AR(10%). The manuscript was written by JL and edited by DL, AB and RvK. All authors read and approved the final manuscript.

Funding

This work was funded by the European Union's Horizon 2020 research and innovation programme under the Marie Skłodowska-Curie grant agreement [H2020-MSCA-CO-FUND 665992]; by Corbion and by the EPSRC [EP/L016354/1].

Declarations of interest

The authors declare no competing interests.

Acknowledgement

We wish to thank Dr. Christopher Ibenegbu and Dr. Alice Marriott for their help. Thanks are also extended to people in the Leak Lab and the Centre for Sustainable Circular Technologies (CSCT) in the University of Bath.

References

Al-Hinai, M. A., Jones, S. W. and Papoutsakis, E. T. 2015. The *Clostridium* sporulation programs: diversity and preservation of endospore differentiation. Microbiology and Molecular Biology Reviews 79, 19–37. https://doi.org/10.1128/MMBR.00025-14.

Aliyu, H., Lebre, P., Blom, J., Cowan, D. and De Maayer, P. 2016. Phylogenomic re-assessment of the thermophilic genus *Geobacillus*. Systematic and Applied Microbiology 39, 527–533. https://doi.org/10.1016/j.syapm.2016.09.004.

Altschul, S. F., Madden, T. L., Schäffer, A. A., Zhang, J., Zhang, Z., Miller, W. and Lipman, D. J. 1997. Gapped BLAST and PSI-BLAST: a new generation of protein database search programs. Nucleic Acids Research 25, 3389–3402. https://doi.org/10.1093/nar/25.17.3389.

Asai, K., Baik, S. H., Kasahara, Y., Moriya, S. and Ogasawara, N. 2000. Regulation of the transport system for C4-dicarboxylic acids in *Bacillus subtilis*. Microbiology 146, 263–271. https://doi.org/10.1099/00221287-146-2-263.

Bacon, L. F., Hamley-Bennett, C., Danson, M. J. and Leak, D. J. 2017. Development of an efficient technique for gene deletion and allelic exchange in *Geobacillus* spp. Microbial Cell Factories 16, 58. https://doi.org/10.1186/s12934-017-0670-4.

Bartosiak-Jentys, J. 2011. *Metabolic engineering and metaboli flux analysis of thermophilic, ethanogenic Geobacillus spp.* (Ph.D. thesis). Imperial College London, UK.

Bartosiak-Jentys, J., Eley, K. and Leak, D. J. 2012. Application of *pheB* as a reporter gene for *Geobacillus* spp., enabling qualitative colony screening and quantitative analysis of promoter strength. Applied and Environmental Microbiology 78, 5945–5947. https://doi.org/10.1128/AEM.07944-11.

Bartosiak-Jentys, J., Hussein, A. H., Lewis, C. J. and Leak, D. J. 2013. Modular system for assessment of glycosyl hydrolase secretion in *Geobacillus thermoglucosidasius*. Microbiology (United Kingdom) 159, 1267–1275. https://doi.org/10.1099/mic.0.066332-0.

Bechthold, I., Bretz, K., Kabasci, S., Kopitzky, R. and Springer, A. 2008. Succinic acid: a new platform chemical for biobased polymers from renewable resources. Chemical Engineering & Technology: Industrial Chemistry-Plant Equipment-Process Engineering-Biotechnology 31, 647–654. https://doi.org/10.1002/ceat.200800063.

Campbell, K., Herrera-Dominguez, L., Correia-Melo, C., Zelezniak, A. and Ralser, M. 2018. Biochemical principles enabling metabolic cooperativity and phenotypic heterogeneity at the single cell level. Current Opinion in Systems Biology 8, 97–108. https://doi.org/10.1016/j.coisb.2017.12.001.

Chang, A. Y., Chau, V., Landas, J. A. and Pang, Y. 2017. Preparation of calcium competent *Escherichia coli* and heat-shock transformation. JEMI Methods 1, 22–25. https://ujemi.microbiology.ubc.ca/node/127.

Chen, C., Lu, Y., Wang, L., Yu, H. and Tian, H. 2018. CcpA-dependent carbon catabolite repression regulates fructooligosaccharides metabolism in *Lactobacillus plantarum*. Frontiers in Microbiology 9, 1114. https://doi.org/10.3389/fmicb.2018.01114.

Conejo, M. S., Thompson, S. M. and Miller, B. G. 2010. Evolutionary bases of carbohydrate recognition and substrate discrimination in the ROK protein family. Journal of Molecular Evolution 70, 545–556. https://doi.org/10.1007/s00239-010-9351-1.

Cuebas, M., Villafane, A., McBride, M., Yee, N. and Bini, E. 2011. Arsenate reduction and expression of multiple chromosomal *ars* operons in *Geobacillus kaustophilus* A1. Microbiology 157, 2004–2011. https://doi.org/10.1099/mic.0.048678-0.

Dahl, M. K. and Hillen, W. 1995. Contributions of Xy1R, CcpA and HPr to catabolite repression of the *xyl* operon in *Bacillus subtilis*. FEMS Microbiology Letters 132, 79–83. https://doi.org/10.1111/j.1574-6968.1995.tb07814.x.

Dahl, M. K., Schmiedel, D. and Hillen, W. 1995. Glucose and glucose-6-phosphate interaction with Xyl repressor proteins from *Bacillus* spp. may contribute to regulation of xylose utilization. Journal of Bacteriology 177, 5467–5472. .

Fujita, Y. 2009. Carbon catabolite control of the metabolic network in *Bacillus sutilis*. Bioscience, Biotechnology and Biochemistry 73, 245–259. https://doi.org/10.1271/bbb.80479.

Galinier, A., Deutscher, J. and Martin-Verstraete, I. 1999. Phosphorylation of either Crh or HPr mediates binding of CcpA to the *Bacillus subtilis xyn cre* and catabolite repression of the *xyn* operon. Journal of Molecular Bbiology 286, 307–314. https://doi.org/10.1006/jmbi.1998.2492.

Görke, B. and Stülke, J. 2008. Carbon catabolite repression in bacteria: Many ways to make the most out of nutrients. Nature Reviews Microbiology 6, 613–624. https://doi.org/10.1038/nrmicro1932.

Grant, S. G., Jessee, J., Bloom, F. R. and Hanahan, D. 1990. Differential plasmid rescue from transgenic mouse dnas into *Escherichia coli* methylation-restriction mutants. Proceedings of the National Academy of Sciences 87, 4645–4649. https://doi.org/10.1073/pnas.87.12.4645.

Hills, C. A. 2015. *Acetate metabolism in Geobacillus thermoglucosidasius and strain engineering for enhanced bioethanol production* (Ph.D. thesis, University of Bath, UK). https://researchportal.bath.ac.uk/en/studentTheses/acetate-metabolism-in-geobacillus-thermoglucosidasius-and-strain-.

Hueck, C. J. and Hillen, W. 1995. Catabolite repression in *Bacillus subtilis*: a global regulatory mechanism for the Gram-positive bacteria? Molecular Microbiology 15, 395–401. https://doi.org/10.1111/j.1365-2958.1995.tb02252.x.

Hussein, A. H., Lisowska, B. K. and Leak, D. J. 2015. *The Genus Geobacillus and Their Biotechnological Potential* (Vol. 92). Advances in Applied Microbiology. https://doi.org/10.1016/bs.aambs.2015.03.001.

Inácio, J. M., Costa, C. and de Sá-Nogueira, I. 2003. Distinct molecular mechanisms involved in carbon catabolite repression of the arabinose regulon in *Bacillus subtilis*. Microbiology 149, 2345–2355. https://doi.org/10.1099/mic.0.26326-0.

Ishida, T., Kita, A., Miki, K., Nozaki, M. and Horiike, K. 2002. Structure and reaction mechanism of catechol 2, 3-dioxygenase (metapyrocatechase). In *International congress series* (Vol. 1233, pp. 213–220). Elsevier. https://doi.org/10.1016/S0531-5131(02)00149-8.

Isikgor, F. H. and Becer, C. R. 2015. Lignocellulosic biomass: a sustainable platform for the production of bio-based chemicals and polymers. Polymer Chemistry 6, 4497–4559. https://doi.org/10.1039/C5PY00263J.

Jones, C. R., Ray, M. and Strobel, H. J. 2002. Transcriptional analysis of the xylose ABC transport operons in the thermophilic anaerobe Thermoanaerobacter ethanolicus. Current Microbiology 45, 54–62. https://doi.org/10.1007/s00284-001-0099-0.

Junker, B., Lester, M., Leporati, J., Schmitt, J., Kovatch, M., Borysewicz, S., ... others 2006. Sustainable reduction of bioreactor contamination in an industrial fermentation pilot plant. Journal of Bioscience and Bioengineering 102, 251–268. https://doi.org/10.1263/jbb.102.251.

Kim, J. H., Block, D. E. and Mills, D. A. 2010. Simultaneous consumption of pentose and hexose sugars: An optimal microbial phenotype for efficient fermentation of lignocellulosic biomass. Applied Microbiology and Biotechnology 88, 1077–1085. https://doi.org/10.1007/s00253-010-2839-1.

Kim, J. H., Shoemaker, S. P. and Mills, D. A. 2009. Relaxed control of sugar utilization in *Lactobacillus brevis*. Microbiology 155, 1351–1359. https://doi.org/10.1099/mic.0.024653-0.

Koide, A., Perego, M. and Hoch, J. A. 1999. ScoC regulates peptide transport and sporulation initiation in *Bacillus subtilis*. Journal of Bacteriology 181, 4114–4117. https://doi.org/10.1128/JB.181.13.4114-4117.1999.

Kraus, A., Hueck, C., Gartner, D. and Hillen, W. 1994. Catabolite repression of the *Bacillus subtilis xyl* operon involves a cis element functional in the context of an unrelated sequence, and glucose exerts additional xylR-dependent repression. Journal of Bacteriology 176, 1738–1745. https://doi.org/10.1128/jb.176.6.1738-1745.1994.

Krispin, O. and Allmansberger, R. 1998. The *Bacillus subtilis* AraE protein displays a broad substrate specificity for several different sugars. Journal of Bacteriology 180, 3250–3252. https://doi.org/10.1128/JB.180.12.3250-3252.1998.

Li, F.-F., Zhao, Y., Li, B.-Z., Qiao, J.-J. and Zhao, G.-R. 2016. Engineering *Escherichia coli* for production of 4-hydroxymandelic acid using glucose-xylose mixture. Microbial Cell Factories 15, 1–11. https://doi.org/10.1186/s12934-016-0489-4.

Lin, L., Song, H., Tu, Q., Qin, Y., Zhou, A., Liu, W., ... Xu, J. 2011. The Thermoanaerobacter glycobiome reveals mechanisms of pentose and hexose co-utilization in bacteria. PLoS Genetics 7, . https://doi.org/10.1371/journal.pgen.1002318.

Lin, P. P., Rabe, K. S., Takasumi, J. L., Kadisch, M., Arnold, F. H. and Liao, J. C. 2014. Isobutanol production at elevated temperatures in thermophilic *Geobacillus thermoglucosidasius*. Metabolic Engineering 24, 1–8. https://doi.org/10.1016/j.ymben.2014.03.006.

Liu, C. G., Lin, Y. H. and Bai, F. W. 2011. Development of redox potential-controlled schemes for very-high-gravity ethanol fermentation. Journal of Biotechnology 153, 42–47. https://doi.org/10.1016/j.jbiotec.2011.03.007.

Loftie-Eaton, W., Taylor, M., Horne, K., Tuffin, M. I., Burton, S. G. and Cowan, D. A. 2013. Balancing redox cofactor generation and ATP synthesis: key microaerobic responses in thermophilic fermentations. Biotechnology and Bioengineering 110, 1057–1065. https://doi.org/10.1002/bit.24774.

Macklyne, H.-R. V. 2017. *Engineering bacteria for biofuel production* (Ph.D. thesis, University of Sussex, UK). http://sro.sussex.ac.uk/id/eprint/67293.

Miwa, Y., Nakata, a., Ogiwara, a., Yamamoto, M. and Fujita, Y. 2000. Evaluation and characterization of catabolite-responsive elements (*cre*) of *Bacillus subtilis*. Nucleic Acids Research 28, 1206–10. https://doi.org/10.1093/nar/28.5.1206.

Mohkam, M., Nezafat, N., Berenjian, A., Mobasher, M. A. and Ghasemi, Y. 2016. Identification of *Bacillus* probiotics isolated from soil rhizosphere using 16S rRNA, *recA*, *rpoB* gene sequencing and RAPD-PCR. Probiotics and Antimicrobial Proteins 8, 8–18. https://doi.org/10.1007/s12602-016-9208-z.

Nozaki, M., Kotani, S., Ono, K. and Senoh, S. 1970. Metapyrocatechase III. Substrate specificity and mode of ring fission. Biochimica et Biophysica Acta - Enzymology 220, 213–223. https://doi.org/10.1016/0005-2744(70)90007-0.

OpenWetWare. 2013. *Choosing Primers for qPCR.* Retrieved from https://bit.ly/3xiH1oT (accessed 16 January 2020)

Park, Y.-C., Jun, S. Y. and Seo, J.-H. 2012. Construction and characterization of recombinant *Bacillus subtilis* JY123 able to transport xylose efficiently. Journal of Biotechnology 161, 402–406. https://doi.org/10.1016/j.jbiotec.2012.07.192.

Pogrebnyakov, I., Jendresen, C. B. and Nielsen, A. T. 2017. Genetic toolbox for controlled expression of functional proteins in *Geobacillus* spp. PLoS ONE 12, 1–15. https://doi.org/10.1371/journal.pone.0171313.

Puri-Taneja, A., Paul, S., Chen, Y. and Hulett, F. M. 2006. CcpA causes repression of the phoPR promoter through a novel transcription start site, PA6. Journal of Bacteriology 188, 1266–1278. https://doi.org/10.1128/JB.188.4.1266-1278.2006.

Radonić, A., Thulke, S., Mackay, I. M., Landt, O., Siegert, W. and Nitsche, A. 2004. Guideline to reference gene selection for quantitative real-time PCR. Biochemical and Biophysical Research Communications 313, 856–862. https://doi.org/10.1016/j.bbrc.2003.11.177.

Raita, M., Ibenegbu, C., Champreda, V. and Leak, D. J. 2016. Production of ethanol by thermophilic oligosaccharide utilising *Geobacillus thermoglucosidasius* TM242 using palm kernel cake as a renewable feedstock. Biomass and Bioenergy 95, 45–54. https://doi.org/10.1016/j.biombioe.2016.08.015.

Reeve, B., Martinez-Klimova, E., de Jonghe, J., Leak, D. J. and Ellis, T. 2016. The *Geobacillus* plasmid set: a modular toolkit for thermophile engineering. ACS Synthetic Biology 5, 1342–1347. https://doi.org/10.1021/acssynbio.5b00298.

Rodionov, D. A., Mironov, A. A. and Gelfand, M. S. 2001. Transcriptional regulation of pentose utilisation systems in the *Bacillus/Clostridium* group of bacteria. FEMS Microbiology Letters 205, 305–314. https://doi.org/10.1111/j.1574-6968.2001.tb10965.x.

Shaw, A. J., Podkaminer, K. K., Desai, S. G., Bardsley, J. S., Rogers, S. R., Thorne, P. G., ... Lynd, L. R. 2008. Metabolic engineering of a thermophilic bacterium to produce ethanol at high yield. Proceedings of the National Academy of Sciences 105, 13769–13774. https://doi.org/10.1073/pnas.0801266105.

Sheng, L., Kovács, K., Winzer, K., Zhang, Y. and Minton, N. P. 2017. Development and implementation of rapid metabolic engineering tools for chemical and fuel production in *Geobacillus thermoglucosidasius* NCIMB 11955. Biotechnology for Biofuels 10, 1–18. https://doi.org/10.1186/s13068-016-0692-x.

Singh, K. D., Schmalisch, M. H., Stülke, J. and Görke, B. 2008. Carbon catabolite repression in *Bacillus subtilis*: Quantitative analysis of repression exerted by different carbon sources. Journal of Bacteriology 190, 7275–7284. https://doi.org/10.1128/JB.00848-08.

Stabb, E. V. and Ruby, E. G. 2002. Rp4-based plasmids for conjugation between escherichia coli and members of the vibrionaceae. Methods in Enzymology 358, 413–426. https://doi.org/10.1016/S0076-6879(02)58106-4.

Tang, Y. J., Sapra, R., Joyner, D., Hazen, T. C., Myers, S., Reichmuth, D., ... Keasling, J. D. 2009. Analysis of metabolic pathways and fluxes in a newly discovered thermophilic and ethanol-tolerant *Geobacillus* strain. Biotechnology and Bioengineering 102, 1377–1386. https://doi.org/10.1002/bit.22181.

VanFossen, A. L., Verhaart, M. R., Kengen, S. M. and Kelly, R. M. 2009. Carbohydrate utilization patterns for the extremely thermophilic bacterium Caldicellulosiruptor saccharolyticus reveal broad growth substrate preferences. Applied and Environmental Microbiology 75, 7718–7724. https://doi.org/10.1128/AEM.01959-09.

Van Kranenburg, R., Verhoef, A. and Machielsen, M. P. 2019. *Genetic modification of (s)-lactic acid producing thermophilic bacteria.* https://patentscope.wipo.int/search/en/detail.jsf?docId=WO2016012298. United States Patent. (US Patent 10,273,509)

Vemuri, G. N., Altman, E., Sangurdekar, D., Khodursky, A. B. and Eiteman, M. A. 2006. Overflow metabolism in *Escherichia coli* during steady-state growth: transcriptional regulation and effect of the redox ratio. Applied and Environmental Microbiology 72, 3653–3661. https://doi.org/10.1128/AEM.72.5.3653-3661.2006.

Vinuselvi, P., Kim, M. K., Lee, S. K. and Ghim, C. M. 2012. Rewiring carbon catabolite repression for microbial cell factory. BMB Reports 45, 59–70. https://doi.org/10.5483/BMBRep.2012.45.2.59.

Warner, J. B. and Lolkema, J. S. 2003a. CcpA-dependent carbon catabolite repression in bacteria. Microbiology and Molecular Biology Reviews 67, 475–490. https://doi.org/10.1128/MMBR.67.4.475-490.2003.

Warner, J. B. and Lolkema, J. S. 2003b. A Crh-specific function in carbon catabolite repression in *Bacillus subtilis*. FEMS Microbiology Letters 220, 277–280. https://doi.org/10.1016/S0378-1097(03)00126-5.

Whitfield, M. B., Chinn, M. S. and Veal, M. W. 2012. Processing of materials derived from sweet sorghum for biobased products. Industrial Crops and Products 37, 362–375. https://doi.org/10.1016/j.indcrop.2011.12.011.

Zhang, B., Li, X.-l., Fu, J., Li, N., Wang, Z., Tang, Y.-j. and Chen, T. 2016. Production of acetoin through simultaneous utilization of glucose, xylose, and arabinose by engineered *Bacillus subtilis*. PLoS One 11, e0159298. https://doi.org/10.1371/journal.pone.0159298.

Appendix

A Correlation curve of cell dry weight and OD_{600}

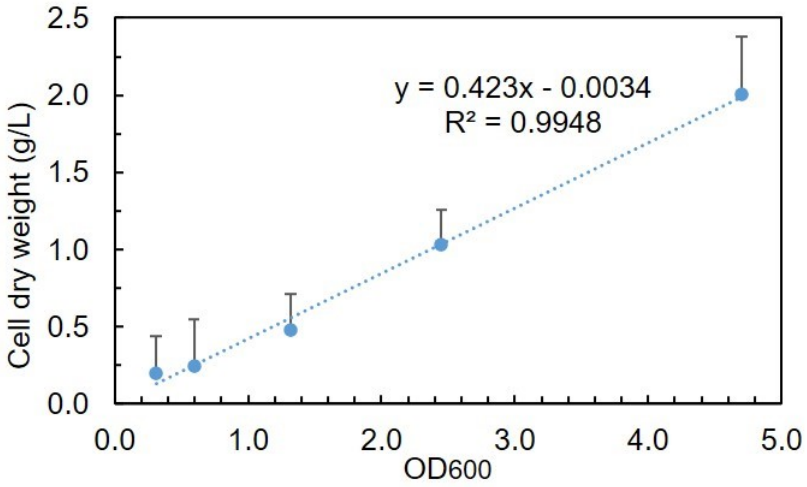

Figure A.1: Calibration curve for relationship between OD_{600} and cell dry weight (g/L) in *P. thermoglucosidasius* DSM 2542. Error bars are standard deviation of three technical replicates for each condition.